

A COMPREHENSIVE COMPARISON OF THE SUN TO OTHER STARS: SEARCHING FOR SELF-SELECTION EFFECTS

JOSÉ A. ROBLES¹, CHARLES H. LINEWEAVER¹, DANIEL GRETHER², CHRIS FLYNN³, CHAS A. EGAN^{2,4}, MICHAEL B. PRACY⁴, JOHAN HOLMBERG⁵ AND ESKO GARDNER³

Received 2007 December 21; accepted 2008 May 10

ABSTRACT

If the origin of life and the evolution of observers on a planet is favoured by atypical properties of a planet’s host star, we would expect our Sun to be atypical with respect to such properties. The Sun has been described by previous studies as both typical and atypical. In an effort to reduce this ambiguity and quantify how typical the Sun is, we identify 11 maximally-independent properties that have plausible correlations with habitability, and that have been observed by, or can be derived from, sufficiently large, currently available and representative stellar surveys. By comparing solar values for the 11 properties, to the resultant stellar distributions, we make the most comprehensive comparison of the Sun to other stars. The two most atypical properties of the Sun are its mass and orbit. The Sun is more massive than $95 \pm 2\%$ of nearby stars and its orbit around the Galaxy is less eccentric than $93 \pm 1\%$ of FGK stars within 40 parsecs. Despite these apparently atypical properties, a χ^2 -analysis of the Sun’s values for 11 properties, taken together, yields a solar $\chi^2_{\odot} = 8.39 \pm 0.96$. If a star is chosen at random, the probability that it will have a lower value (\sim be more typical) than the Sun, with respect to the 11 properties analyzed here, is only $29 \pm 11\%$. These values quantify, and are consistent with, the idea that the Sun is a typical star. If we have sampled all reasonable properties associated with habitability, our result suggests that there are no special requirements for a star to host a planet with life.

Subject headings: stars: fundamental parameters — stars: statistics — Sun: fundamental parameters — Sun: general

1. INTRODUCTION

If the properties of the Sun are consistent with the idea that the Sun was randomly selected from all stars, this would indicate that life needs nothing special from its host star and would support the idea that life may be common in the universe. More particularly, if there is nothing special about the Sun, we have little reason to limit our life-hunting efforts to planets orbiting Sun-like stars. As an example of the type of anthropic reasoning we are using, consider the following situation. Suppose uranium (a low abundance element in the Solar System and in the universe) was central to the biochemistry of life on Earth. Further, suppose that a comparison of our Sun to other stars showed that the Sun had more uranium than any other star. How should we interpret this fact? The most reasonable way to proceed would be to try to evaluate the probability that such a coincidence happened by chance and to determine whether we are justified in reading some importance into it. Although a correlation does not necessarily imply cause, we think that a correlation between the Sun’s anomalous feature and life’s fundamental chemistry would be giving us important clues about the conditions necessary for life. Specifically, the search for life around other stars

as envisioned by the NASA’s Terrestrial Planet Finder or ESA’s Darwin Project and as currently underway with SETI would change the strategy to focus on the most uranium-rich stars. Another example: Suppose the Sun had the highest [Fe/H] of all the stars that had ever been observed. Then high [Fe/H] would be strongly implicated as a precondition for our existence, possibly by playing a crucial role in terrestrial planet formation. These are exaggerated examples of the more subtle correlations that a detailed and comprehensive comparison of the Sun with other stars could reveal.

Whether the Sun is a typical or atypical star with respect to 1 or a few properties has been addressed in previous studies. Using an approach similar to ours (comparing solar to stellar properties from particular samples), some studies have suggested that the Sun is a typical star (Gustafsson 1998; Allende Prieto 2006), while other studies have suggested that the Sun is an atypical star (Gonzalez 1999a,b; Gonzalez et al. 2001). This apparent disagreement arises from three problems:

1. Language used to describe whether the Sun is, or is not typical, is often confusingly qualitative. For example, reporting the Sun as “metal-rich”, can mean that the Sun is *significantly* more metal-rich than other stars (e.g. more metal-rich than 80% of other stars) or it can mean that the Sun is *insignificantly* metal-rich (e.g. more metal-rich than 51% of other stars).
2. Selection effects: Stellar samples chosen for the comparison can be biased with respect to the property of interest.

¹ Planetary Science Institute, Research School of Astronomy & Astrophysics and Research School of Earth Sciences, The Australian National University, Canberra Australia; josan@mso.anu.edu.au.

² University of New South Wales, Sydney, Australia.

³ Tuorla Observatory, University of Turku, Finland.

⁴ Research School of Astronomy & Astrophysics, The Australian National University, Canberra, Australia.

⁵ Max Planck Institute for Astronomy, Heidelberg, Germany.

3. Inclusion (or exclusion) of stellar properties for which it is suspected or known that the Sun is atypical, will make the Sun appear more atypical (or typical).

In this paper we address problem 1 by using only quantitative measures when comparing the Sun’s properties to other stars. Our main interest is to move beyond the qualitative assessment of the Sun as either typical or atypical, and obtain a more precise quantification of the degree of the Sun’s (a)typicality. In other words, we want to answer the question ‘How typical is the Sun?’ rather than ‘Is the Sun typical or not?’ There are at least two ways to quantify how typical the Sun is. This can be done for individual parameters by determining how many stars have values below or above the solar value (Table 3). This can also be done by a joint analysis of multiple parameters (Table 2). If there are several subtle factors that have some influence over habitability, a quantitative joint analysis of the Sun’s properties may allow us to identify these factors without invoking largely speculative arguments linking specific properties to habitability.

With respect to problem 2, most previous analyses have compared the Sun to subsets of Sun-like stars selected to be Sun-like with respect to 1 or more parameters. In such analyses, the Sun will appear typical with respect to any parameter(s) correlated with 1 of the pre-selected Sun-like parameters. For example, elemental abundances $[X/H]$ are correlated with metallicity⁶ $[Fe/H]$. The sample of Edvardsson et al. (1993a) was selected to have a wide range of $[Fe/H]$. This produced a metallicity distribution unrepresentative of stars in general. Recognizing this, Edvardsson et al. (1993a) conditioned on solar metallicity, $[Fe/H] \approx 0$ and then compared solar abundances for 12 elements to the abundances in a group of nearby stars with solar iron abundance, solar age and solar galactocentric radius. They found the Sun to be “a quite typical star for its metallicity, age and galactic orbit”. Similarly, Gustafsson (1998), after comparing various properties of the Sun to solar-type stars (stars of similar mass and age), concluded that the Sun seems very normal for its mass and age; “The Sun, to a remarkable degree, is solar type”. The stellar samples we use for comparison with the Sun are, in our judgement, the least-biased samples currently available for such a comparison.

To address problem 3, in Section 2 we compare the Sun to other stars using a large number (11) of maximally-independent properties with plausible correlations with habitability. These properties can be observed or derived for a sufficiently large, representative stellar sample (Table 1). Any property of the Sun or its environment which must be special to allow habitability would show up in our analysis. However, in contrast to previous analyses which have looked for solar anomalies with respect to individual properties, we perform a joint analysis that enables us to quantify how typical the solar values are, taken as a group. In Section 3, the differences between the solar values and the stellar samples’ medians are used to perform first a simple and then an improved version

of a χ^2 -analysis to estimate whether the solar values are characteristic of a star selected at random from the stellar samples. The results of our joint analysis are presented in Figure 13 of Section 4. We find that the solar values, taken as a group, are consistent with the Sun being a random star. However, there are important caveats to this interpretation associated with the compromise between the number of properties analyzed, and their plausibility of being correlated with habitability. In Sections 5 and 6 we discuss these caveats and summarize. We discuss the levels of correlation between our 11 properties in Appendix A.

2. STELLAR SAMPLES AND SOLAR VALUES

We are looking for a signal associated with a prerequisite for, or a property that favors, the origin and evolution of life (see Gustafsson 1998 for a brief discussion of this idea). If we indiscriminately include many properties with little or no plausible correlation with habitability, we run the risk of diluting any potential signal. If we choose only a few properties based on previous knowledge that the Sun is anomalous with respect to those properties, we are making a useful quantification but we are unable to address problem *iii*. We choose a middle ground and try to identify as many properties as we can that have some plausible association with habitability. This strategy is most sensitive if a few unknown stellar properties (among the ones being tested) contribute to the habitability of a terrestrial planet in orbit around a star.

An optimal quantitative comparison of the Sun to other stars would require an unbiased, large representative stellar sample from which independent distributions, for as many properties as desired, could be compared. Such a distribution for each property of interest would allow a straightforward analysis and outcome: the Sun is within the $n\%$ of stars around the centroid of the N -dimensional distribution. However, observational and sample selection effects prevent the assembly of such an ideal stellar sample.

In this study, we compare the Sun to other stars with respect to the following 11 basic physical properties: (1) mass, (2) age, (3) metallicity $[Fe/H]$, (4) carbon-to-oxygen ratio $[C/O]$, (5) magnesium-to-silicon ratio $[Mg/Si]$, (6) rotational velocity $v \sin i$, (7) eccentricity of the star’s galactic orbit e , (8) maximum height to which the star rises above the galactic plane Z_{\max} , (9) mean galactocentric radius R_{Gal} , (10) the mass of the star’s host galaxy M_{gal} , (11) the mass of the star’s host group of galaxies M_{group} . These 11 properties span a wide range of stellar and galactic factors that may be associated with habitability. We briefly discuss how each parameter might have a plausible correlation with habitability. For each property we have tried to assemble a large, representative sample of stars whose selection criteria is minimally biased with respect to that property. For each property the percentage of stars with values lower and higher than the solar value are computed. For properties (9), (10) and (11), the uncertainties in the percentages are determined from the uncertainties of the distributions. For the rest of the properties, nominal uncertainties Δ , on the percentages were calculated assuming a binomial distribution (*e.g.* Mever

⁶ Metallicity: $[Fe/H]$ is the fractional abundance of Fe rel-

TABLE 1
 SAMPLES USED TO PRODUCE THE STELLAR DISTRIBUTIONS PLOTTED IN FIG.

Figure	Property	Range	Med $\mu_{1/2}$
1	Mass [M_{\odot}]	0.08 – 2	0.3
2	Age [Gyr]	0 – 15	5.
3	[Fe/H]	-1.20 – +0.46	-0.
4A	[C/O]	-0.22 – +0.32	0.0
4B	[Mg/Si]	-0.18 – +0.14	0.0
5	$v \sin i$ [km s^{-1}]	0 – 36	2.5
6	e	0 – 1	0.1
7	Z_{max} [kpc]	0 – 9.60	0.1
8	R_{Gal} [kpc]	0 – 30	4.
9	M_{gal} [M_{\odot}] ^k	10^7 – 10^{12}	10^{10}
10	M_{group} [M_{\odot}] ^k	10^9 – 10^{13}	10^{11}

† Characteristic width of distribution in the direction of the solar value.

- †
^a Wright et al. (2004), (see footnote in Sec. 2.2).
^b G99: Gustafsson et al. 1999, R03: Reddy et al. 2003, BF06: Bensby & Feltzing 2006.
^c R03: Reddy et al. 2003, B05: Bensby et al. 2005.
^d Solar rotational velocity corrected for random inclination (see Sec. 2.5).
^e Sub-set of stars within the mass range: $0.9 M_{\odot} \leq M \leq 1.1 M_{\odot}$.
^f Calculated using the solar galactic motion (Dehnen & Binney 1998) and the Galactic potential (see Sec. 2.6).
^g Sub-set of volume complete A5–K2 stars within 40 pc.
^h Integrated solar orbit in the Galactic potential of Flynn et al. (1996) (see Sec. 2.6).
ⁱ Eisenhauer et al. 2005.
^j BS80: Bahcall & Soneira 1980, G96: Gould et al. 1996, E05: Eisenhauer et al. 2005.
^k Stellar mass, not total baryonic mass, nor total mass.
^l D94: Driver et al. 1994, CB99: Courteau & van den Bergh 1999, L00: Loveday 2000, BJ01: Bell & de Jong 2001, J03: Jarrett et al. 2003.

the fraction of stars with a lower (higher) value than the Sun and N_{tot} is the total number of stars in the sample. The solar value is indicated with the symbol “ \odot ” in all figures.

We compare the Sun and its environment to other stars and their environments. The analysis of these larger environmental contexts provides information about properties that otherwise could not be directly measured. For example, suppose the metallicity of the Sun were normal with respect to stars in the solar neighborhood but that these stars as a group, had an anomalously high metallicity with respect to the average metallicity of stars in the Universe. This fact would strongly suggest that habitability is associated with high metallicity, but our comparison with only local stars would not pick this up. In the absence of an [Fe/H] distribution for all stars in the Universe, we use galactic mass as a convenient proxy for any such property that correlates with galaxy mass.

2.1. Mass

Mass is probably the single most important characteristic of a star. For a main sequence star, mass determines luminosity, effective temperature, main sequence life-time and the dimensions, UV insolation and temporal stability of the circumstellar habitable zone (Kasting et al. 1993).

Low mass stars are intrinsically dim. Thus a complete sample of stars can only be obtained out to a distance of ~ 7 parsecs (≈ 23 lightyears). Figure 1 compares the mass of the Sun to the stellar mass distribution of the 125 nearest main sequence stars within 7.1 pc, as compiled by the RECONS consortium (Henry 2006). Over-plotted is the stellar Initial Mass Function (IMF; see eqs. 4 & 5 and Table 1 of Kroupa 2002) limited to 125 stars more massive than the brown dwarf limit

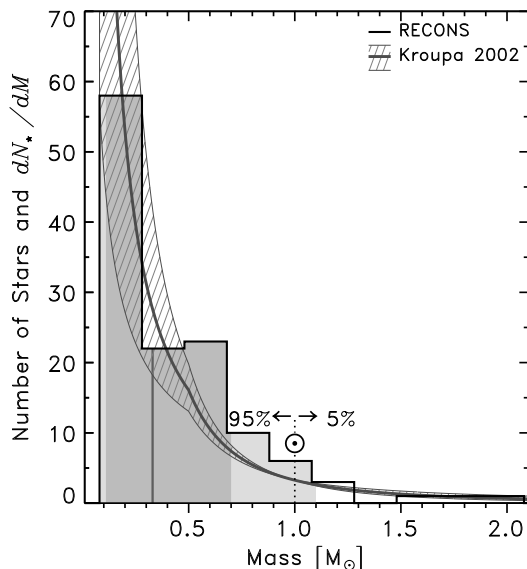


FIG. 1.— Mass histogram of the 125 nearest stars (Henry 2006, RECONS). The median ($\mu_{1/2} = 0.33 M_{\odot}$) of the distribution is indicated by the vertical grey line. The 68% and 95% bands around the median are indicated respectively by the vertical dark grey and light grey bands. We also use these conventions in Figs. 2–11. The solid curve and hashed area around it represents the Initial Mass Function (IMF) and its associated uncertainty (Kroupa 2002). The Sun, indicated by “ \odot ”, is more massive than $95 \pm 2\%$ of these stars.

sal (Kroupa & Weidner 2005), these nearby comparison stars are representative of a much larger sample of stars. There is good agreement between the histogram and the IMF — the Sun is more massive than $95 \pm 2\%$ of the nearest stars, and more massive than $94 \pm 2\%$ of the stars in the Kroupa (2002) IMF. Fourteen brown dwarfs and

sample. Including them yields 94% — the same result obtained from the IMF. Our $95\% \pm 2\%$ result should be compared with the 91% reported by Gonzalez (1999b). The Sun’s mass is the most anomalous of the properties studied here.

2.2. Age

If the evolution of observers like ourselves takes on average many billions of years, we might expect the Sun to be anomalously old (Carter 1983). Accurate estimation of stellar ages is difficult. For large stellar surveys ($>$ a few hundred stars), the most commonly used age indicators are based on isochrone fitting and/or chromospheric activity (R'_{HK} index). Rocha-Pinto et al. (2000b) have estimated a Star Formation Rate (SFR), or equivalently, an age distribution for the local Galactic disk from chromospheric ages of 552 late-type (F8–K2) dwarf stars in the mass range $0.8 M_{\odot} \leq M \leq 1.4 M_{\odot}$ at distances $d \leq 200$ pc (Rocha-Pinto et al. 2000a). They applied scale-height corrections, stellar evolution corrections and volume incompleteness corrections that converted the observed age distribution into the total number of stars born at any given time. Hernandez et al. (2000) and Bertelli & Nasi (2001) have made estimates of the star formation rate in the solar neighborhood and favour a smoother distribution (fewer bursts) than Rocha-Pinto et al. (2000b).

In Figure 2 we compare the chromospheric age of the Sun ($\tau_{\odot} = 4.9 \pm 3.0$ Gyr, Wright et al. 2004)⁷ to the stellar age distribution representing the Galactic SFR (Rocha-Pinto et al. 2000b). The median of this distribution is 5.4 Gyr. The Sun is younger than $53 \pm 2\%$ of the stars in the thin disk of our Galaxy. Over-plotted is the cosmic SFR derived by Hopkins & Beacom (2006). According to this distribution with a median $\mu_{1/2} = 9.15$ Gyr, the Sun was born after $86 \pm 5\%$ of the stars that have ever been born.

The Galactic and cosmic SFRs are different because the cosmic SFR was dominated by bulges and elliptical galaxies in which the largest fraction of stellar mass in the Universe resides. Bulges and elliptical galaxies (early-type galaxies) formed their stars early and quickly and then ran out of gas. The disks of spiral galaxies, like our Milky Way, seem to have undergone irregular bursts of star formation over a longer period of time as they interacted with their satellite galaxies.

The volume limited ($d_{\text{max}} = 40$ pc) sub-set from Nordström et al. (2004) contains isochrone ages for 1126 A5–K2 stars. The median of this sub-set is 5.9 Gyr and the Sun is younger than $55 \pm 2\%$ of the stars. The similarity of this isochrone age result to the chromospheric age result is not obvious since the agreement between these two age techniques is rather poor. This mismatch can be seen in Fig. 15D, Reid et al. (2007), and in Fig. 8 of Feltzing et al. (2001).

2.3. Metallicity

Iron is the most frequently measured element in nearby stars. Metallicity $[\text{Fe}/\text{H}]$, is known to be a proxy for

⁷ To ensure that the Sun’s age is determined in the same way as the stellar ages to which it is being compared, we adopt the

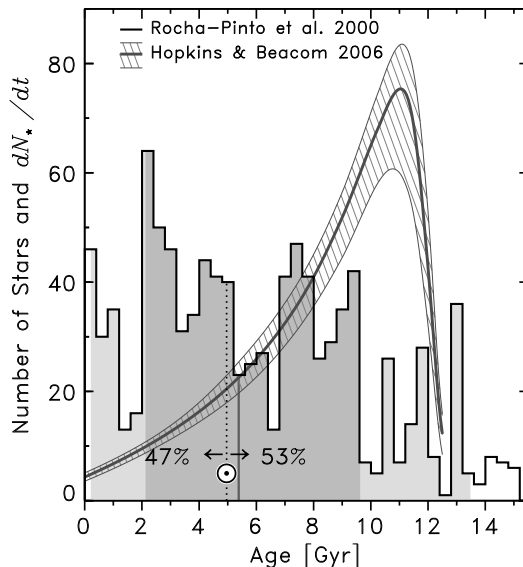


FIG. 2.— The Galactic stellar age distribution (median $\mu_{1/2} = 5.4$ Gyr) from Rocha-Pinto et al. (2000b). The Sun is younger than $53 \pm 2\%$ of the stars in the disk of our Galaxy. The grey curve is the cosmic Star Formation Rate (SFR) with its associated uncertainty (Hopkins & Beacom 2006), according to which the Sun is younger than $86 \pm 5\%$ of the stars in the Universe.

the fraction of a star’s mass that is not hydrogen or helium. In the Sun and possibly in the Universe, the dominant contributors to this mass fraction in order of abundance are: O(44%), C(18%), Fe(10%), Ne(8%), Si(6%), Mg(5%), N(5%), S(3%) (Asplund et al. 2005; Truran & Heger 2005). The corresponding abundances by number are: O(48%), C(26%), Ne(7%), N(6%), Mg(4%), Si(4%), Fe(3%), S(2%). Importantly for this analysis, this short list contains the dominant elements in the composition of terrestrial planets (O, Fe, Si and Mg) and life (C, O, N and S).

Over the last few decades, much effort has gone into determining abundances in nearby stars for a wide range of elements. Stellar elemental abundances for element X are usually normalised to the solar abundance of the same element using a logarithmic abundance scale: $[\text{X}/\text{H}]_{\star} \equiv \log(\text{X}/\text{H})_{\star} - \log(\text{X}/\text{H})_{\odot}$. Hence all solar elemental abundances $[\text{X}/\text{H}]_{\odot}$, are defined as zero. Spectroscopic abundance analyses are usually made differential relative to the Sun by analysing the solar spectrum (reflected by the Moon, asteroids or the telescope dome) in the same way as the spectrum of other stars. In this approach, biases introduced by the assumption of local thermodynamic equilibrium (LTE), largely cancel out for Sun-like stars (Edvardsson et al. 1993b).

A comparison between solar and stellar iron abundances is a common feature of most abundance surveys and most have concluded that the Sun is metal-rich compared to other stars (Gustafsson 1998; Gonzalez 1999a,b). However, for our purposes, the appropriateness of these comparisons depends on the selection criteria of the stellar sample to which the Sun has been compared. Stellar metallicity analyses such as Edvardsson et al. (1993a); Reddy et al. (2003); Nordström et al. (2004); Valenti & Fischer (2005) have stellar samples selected with different purposes in mind, e.g. Edvardsson et al.

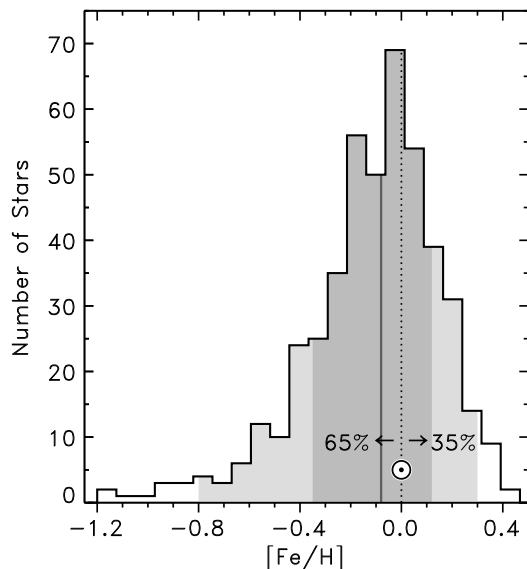


FIG. 3.— Stellar metallicity histogram of the 453 FGK *Hipparcos* stars within 25 pc (Grether & Lineweaver 2007). The median $\mu_{1/2} = -0.08$. The Sun is more metal-rich than $65 \pm 2\%$ of the stars.

the Galaxy and their sample is biased towards low metallicity (average $[\text{Fe}/\text{H}] = -0.25$). The sample of Valenti & Fischer 2005 (average $[\text{Fe}/\text{H}] = -0.01$), was selected as a planet candidate list and contains some bias towards high metallicity (see Grether & Lineweaver 2007). To assess how typical the Sun is, Gustafsson (1998) limited the sample of Edvardsson et al. (1993a) to stars with galactocentric radii within 0.5 kpc of the solar galactocentric radius, and to ages between 4 and 6 Gyrs. The distribution of stars given by this criteria has an average $[\text{Fe}/\text{H}] = -0.09$.

Grether & Lineweaver (2006, 2007) compiled a sample of 453 Sun-like stars within 25 pc. These stars were selected from the *Hipparcos* catalogue, which is essentially complete to 25 pc for stars within the spectral type range F7–K3 and absolute magnitude of $M_V = 8.5$ (Reid 2002). Metallicities for this sample were assembled from a wide range of spectroscopic and photometric surveys. In Figure 3, we compare the Sun to the Grether & Lineweaver (2007) sample, which has a median $[\text{Fe}/\text{H}] = -0.08$. To our knowledge this is the most complete and least-biased stellar spectroscopic metallicity distribution. The Sun is more metal-rich than $65 \pm 2\%$ of these stars.

This result should be compared with Favata et al. (1997) who constructed a volume-limited ($d_{\text{max}} = 25$ pc) sample of 91 G and K dwarfs ranging in color index ($B - V$) between 0.5 – 0.8 (Favata et al. 1996). Their distribution has a median $[\text{Fe}/\text{H}] = -0.05$ and compared to this sample, the Sun is more metal rich than $56 \pm 5\%$ of the stars. Fuhrmann (2008) compared the Sun to a volume complete ($d_{\text{max}} = 25$ pc) sample of about 185 thin-disk mid-F-type to early K-type stars down to $M_V = 6.0$. He finds a mean $[\text{Fe}/\text{H}] = -0.02 \pm 0.18$. This mean $[\text{Fe}/\text{H}]$ is lowered by 0.01 dex if the 43 double-lined spectroscopic binaries in his sample are included. His results are consistent with ours.

The elemental abundance ratios of a host star have a major impact on its proto-planetary disk chemistry and the chemical compositions of its planets. Oxygen and carbon make up $\sim 62\%$ of the solar system’s non-hydrogen-non-helium mass content ($Z = 0.0122$, Asplund et al. 2005). Carbon and oxygen abundances are among the hardest to determine. This is due to high temperature sensitivity and non-LTE effects in their permitted lines (e.g. C I $\lambda 6588$, O I $\lambda 7773$), and to the presence of blends in the forbidden lines ([C I] $\lambda 8727$, [O I] $\lambda 6300$). See Allende Prieto et al. (2001) and Bensby & Feltzing (2006) for details on C and O abundance derivations.

Carbon pairs up with oxygen to form carbon monoxide. In stars with a C/O ratio larger than 1, most of the oxygen condenses into CO which is largely driven out of the incipient circumstellar habitable zone by the stellar wind. In this oxygen-depleted scenario, planets formed within the snow line are formed in reducing environments and are mostly composed of carbon compounds, for example silicon carbide (Kuchner & Seager 2005). Thus, the C/O ratio could be strongly associated with habitability.

As most heavy element abundances relative to hydrogen (e.g. $[\text{O}/\text{H}]$, $[\text{C}/\text{H}]$, $[\text{N}/\text{H}]$) are correlated with $[\text{Fe}/\text{H}]$, they were not included in our analysis. After the overall level of metallicity (represented by $[\text{Fe}/\text{H}]$), and after the ratio of the two most abundant metals, $[\text{C}/\text{O}]$, the magnesium to silicon ratio $[\text{Mg}/\text{Si}]$ is the most important ratio of the next most abundant elements (excluding the noble gas Ne). For example $[\text{Mg}/\text{Si}]$ sets the ratio of olivine to pyroxene which determines the ability of a silicate mantle to retain water (H. O’Neill 2007, private communication).

Stellar elemental abundance ratios are defined as $[X_1/X_2]_{\star} = [X_1/\text{H}]_{\star} - [X_2/\text{H}]_{\star}$. Hence, systematic errors associated with the determination of absolute solar abundances cancel for abundances relative-to-solar. We compile $[\text{C}/\text{O}]$ and $[\text{Mg}/\text{Si}]$ ratios from samples with the largest number of stars and highest signal-to-noise ratio stellar spectra:

$[\text{C}/\text{O}]$.—256 stars from Gustafsson et al. 1999; Reddy et al. 2003; Bensby & Feltzing 2006

$[\text{Mg}/\text{Si}]$.—231 stars from Reddy et al. 2003; Bensby et al. 2005

Due to their selection criteria, these samples are biased towards low metallicity and therefore cannot be used to create a representative $[\text{Fe}/\text{H}]$ distribution. Because a correlation exists between the $[\text{C}/\text{O}]$ and $[\text{Mg}/\text{Si}]$ ratios and $[\text{Fe}/\text{H}]$ (e.g. Gustafsson et al. 1999), the samples we use have a relatively narrow range of $[\text{Fe}/\text{H}]$ to reduce the influence of the correlation. Therefore, these small correlations can be neglected in this study — see the bottom panels of Fig. 4 where $[\text{Fe}/\text{H}]$ versus $[\text{C}/\text{O}]$ as well as $[\text{Fe}/\text{H}]$ versus $[\text{Mg}/\text{Si}]$ are plotted. The top panels show the corresponding stellar distribution histograms. The Sun’s $[\text{C}/\text{O}]$ ratio is lower than $81 \pm 3\%$ of the stars. This is consistent with Gonzalez (1999b) who suggested — based on data from Edvardsson et al. (1993a) and Gustafsson et al. (1999) — that the Sun has a low $[\text{C}/\text{O}]$ ratio relative to Sun-like stars at similar galactocentric

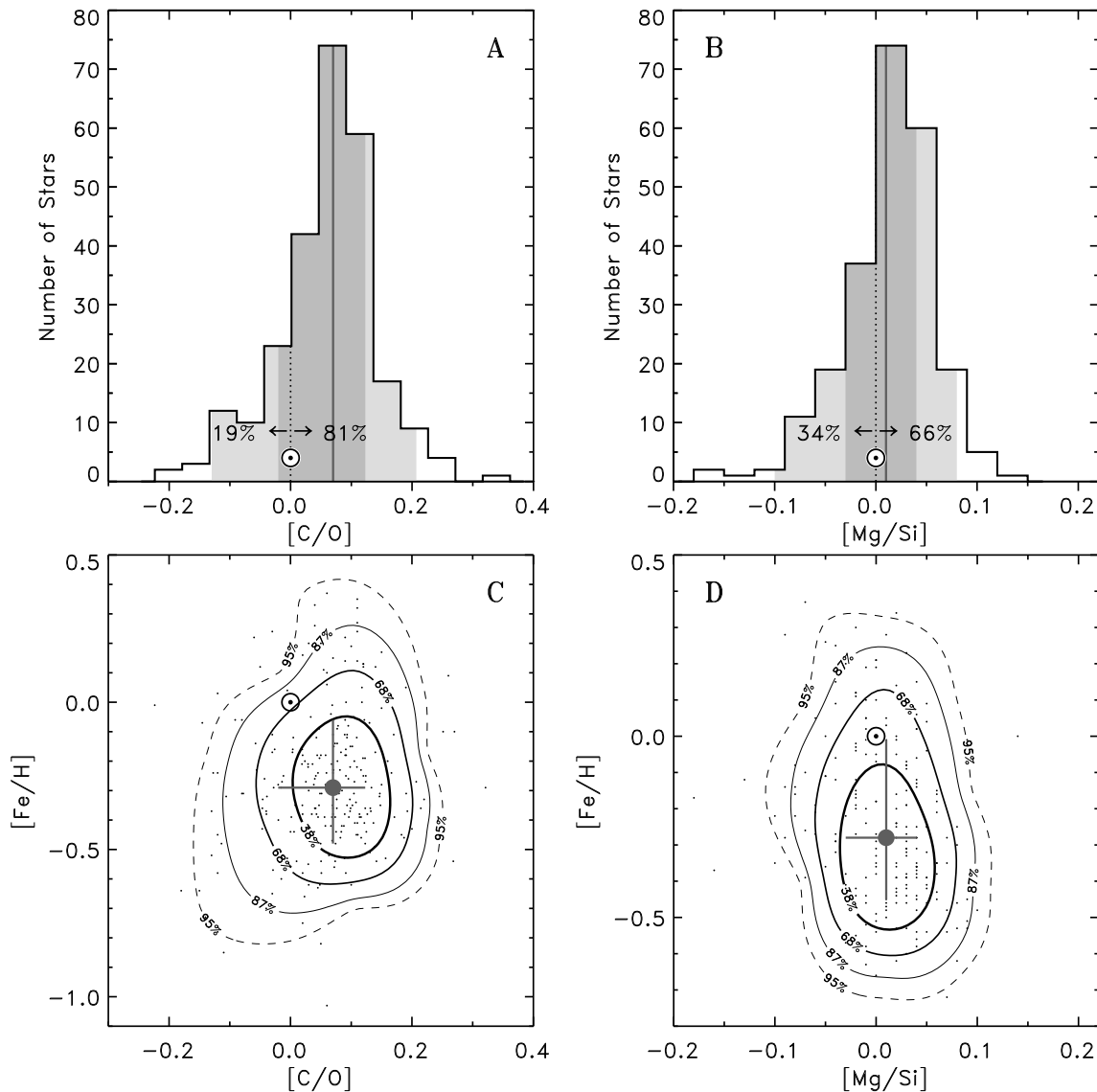


FIG. 4.— **A**: Comparison of the Sun’s carbon-to-oxygen ratio ($[C/O]_{\odot} \equiv 0$) to the $[C/O]$ ratios of 256 stars compiled from Gustafsson et al. (1999); Reddy et al. (2003) and Bensby & Feltzing (2006). The Sun’s $[C/O]$ ratio is lower than $81 \pm 3\%$ of the stars in this sample which has a median $\mu_{1/2} = 0.07$. **B**: Comparison of the Sun’s magnesium-to-silicon ratio ($[Mg/Si]_{\odot} \equiv 0$), to $[Mg/Si]$ values from 231 stars from Reddy et al. (2003) and Bensby et al. (2005). The Sun’s $[Mg/Si]$ ratio is lower than $66 \pm 3\%$ of the stars in this sample with median $\mu_{1/2} = 0.01$. The bottom panels **C** & **D** show the small correlations of these distributions with $[Fe/H]$. These small correlations can be neglected for this study.

the Sun is oxygen poor compared to solar metallicity stars.

The Sun’s $[Mg/Si]$ ratio is lower than $66 \pm 3\%$ of the stars. The $[C/O]$ and $[Mg/Si]$ ratios are also largely independent of each other (see Fig. 14 in Appendix A).

2.5. Rotational Velocity

Stellar rotational velocities are related to the specific angular momentum of a protoplanetary disk and possibly to the magnetic field strength of the star during planet formation, and to protoplanetary disk turbulence and mixing. An unusually low stellar rotational velocity may be associated with the presence of planets (Soderblom 1983). One or several of these factors could be related to habitability.

There is a known correlation between mass and $v \sin i$

(p. 485). In order to minimize the effect of this correlation (and maximize independence between parameters), we assembled a sample containing 276 stars within the mass range $0.9\text{--}1.1 M_{\odot}$ (F8–K2) from Valenti & Fischer (2005). The selection criteria of the Valenti & Fischer (2005) stars introduces some bias against more active stars. We compared the high $v \sin i$ tail of our Valenti & Fischer (2005) sample with the high $v \sin i$ tail of a sub-sample from Nordström et al. (2004). We estimate that for our Valenti & Fischer (2005) sample, the bias introduced by the selection criteria is lower than $\sim 5\%$. The $v \sin i$ values in Valenti & Fischer (2005) are obtained by fixing the macroturbulence for the stars of a given color, without modeling the stars individually. If the macroturbulence value was underestimated for $T > 5800$ K, the resulting $v \sin i$ values (especially

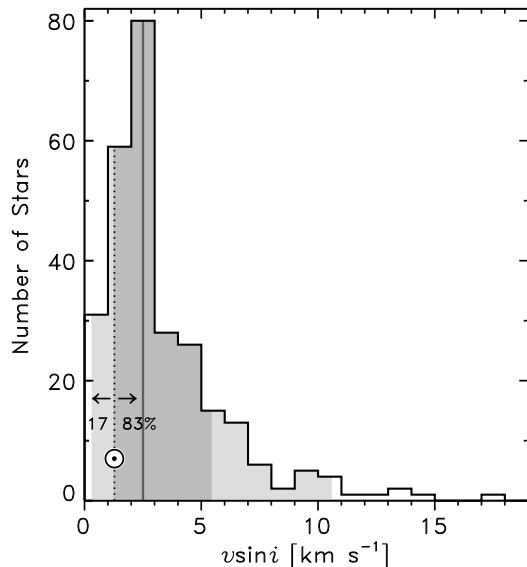


FIG. 5.— Rotational velocity histogram for 276 F8–K2 ($0.9 \leq M \leq 1.1 M_{\odot}$) stars (Valenti & Fischer 2005). The Sun ($v \sin i_{\odot} = 1.28 \text{ km s}^{-1}$) rotates more slowly than $83 \pm 7\%$ of the stars. There is 1 star to the right of the plot with $v \sin i = 36 \text{ km s}^{-1}$.

of Valenti & Fischer 2005).

The inclination of the stellar rotational axis to the line of sight is usually unknown so the observable is $v \sin i$. Using the solar spectrum reflected by the asteroid Vesta, Valenti & Fischer (2005) derived a solar $v \sin i = 1.63 \text{ km s}^{-1}$. For the purposes of this analysis we use the mean value that would be derived for the Sun, when viewed from a random inclination: $v \sin i_{\odot} = 1.63(\pi/4) \text{ km s}^{-1} \approx 1.28 \text{ km s}^{-1}$.

The Sun rotates more slowly than $83 \pm 7\%$ of the stars in our Valenti & Fischer (2005) sample (Fig. 5). This is in agreement with Soderblom (1983, 1985) who reported that the Sun is within 1 standard deviation of stars of its mass and age.

2.6. Galactic Orbital Parameters

The Galactic velocity components of a star (U, V, W) with respect to the local standard of rest (LSR) may be used to compute a star’s orbit in the Galaxy. How typical or atypical is the solar orbit compared to the orbits of other nearby stars in the Galaxy? The orbit may be related to habitability because more eccentric orbits bring a star closer to the Galactic center where there is a larger danger to life from supernovae explosions, cosmic gamma and X-ray radiation and any factors associated with higher stellar densities (Gonzalez et al. 2001; Lineweaver et al. 2004).

For a standard model of the Galactic potential, Nordström et al. (2004) computed orbital parameters for the Sun, and for a large sample (~ 16700) of A5–K2 stars. Their adopted components of the solar velocity relative to the local standard of rest were $(U, V, W) = (10.0 \pm 0.4, 5.25 \pm 0.62, 7.17 \pm 0.38) \text{ km s}^{-1}$ (Dehnen & Binney 1998).

For each of the 1987 stars within 40 pc in the Nordström et al. (2004) catalog, an inner and outer radii R_{\min} and R_{\max} were computed. This yielded the orbital eccentricity $e = (R_{\max} - R_{\min}) / (R_{\max} + R_{\min})$.

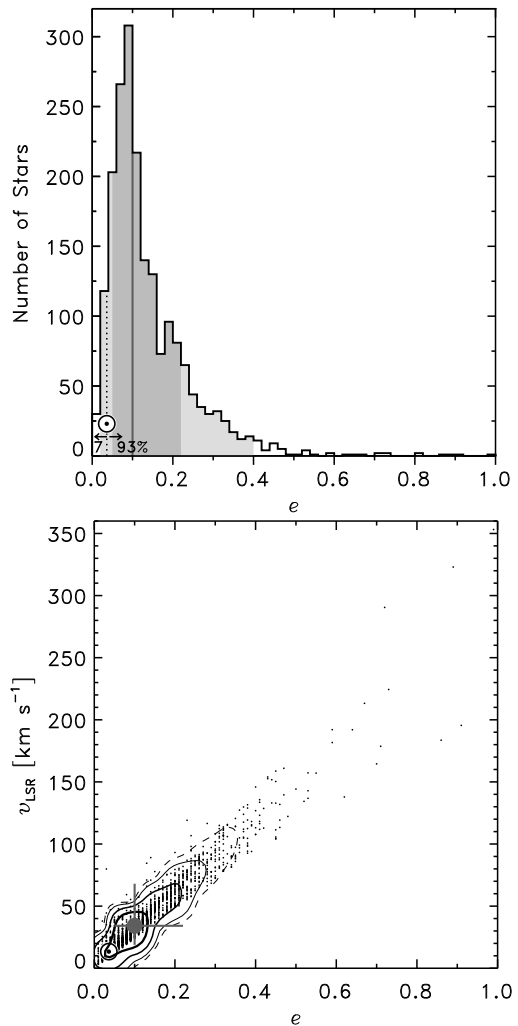


FIG. 6.— Top: eccentricity distribution for the 1,987 stars at $d \leq 40 \text{ pc}$ from Nordström et al. (2004). The Sun has a more circular orbit than $93 \pm 1\%$ of the A5–K2 stars within 40 pc. After mass, eccentricity is the second most anomalous parameter. Bottom panel: Correlation between v_{LSR} and eccentricity for the same stars presented in the Bottom: since these properties are highly correlated we select only 1 for the analysis. The large grey point with error bars represents the median and the 68% widths of the two one-dimensional distributions. As in Fig. 4 the contours correspond to 38%, 68%, 82% and 95%.

nents of the solar motion (Dehnen & Binney 1998) relative to the local standard of rest in the Galactic potential of Flynn et al. (1996). The bottom panel of Figure 6 shows the correlation between Galactic orbital eccentricity e and the magnitude of the galactic orbital velocities with respect to the local standard of rest: $v_{\text{LSR}} \equiv (U^2 + V^2 + W^2)^{1/2}$. Eccentricity e and v_{LSR} are strongly correlated. We include e , not v_{LSR} , in the analysis since e is less correlated with the maximum height above the Galactic plane Z_{\max} , than is v_{LSR} . This is shown in Fig. 16 in Appendix A.

The Sun’s eccentricity was determined with the same relation as the stellar eccentricities. The uncertainty in our estimate of solar eccentricity came from propagating the uncertainty in the adopted solar motion. We find $e_{\odot} = 0.036 \pm 0.002$ (consistent with the $e_{\odot} = 0.043 \pm 0.016$ found by Metzger et al. 1998). The Sun has a more

40 pc (with median eccentricity $\mu_{1/2} = 0.1$). This is the second most anomalous of the 11 solar properties we consider here.

The frequency of the passage of a star through the thin disk could be associated with Galactic gravitational tidal perturbations of Oort cloud objects that might increase the impact rate on potentially habitable planets. This is correlated with the maximum height, Z_{\max} , to which the stars rise above the Galactic plane. Figure 7 shows the stellar distribution of Z_{\max} for the stars shown in Figure 6. We find that $59 \pm 3\%$ of the A5–K2 stars within 40 pc of the Sun reach higher above the Galactic plane than the Sun does ($Z_{\max, \odot} = 0.104 \pm 0.006$ kpc). The solar $Z_{\max, \odot}$ was derived by integrating the solar orbit in the Galactic potential. The uncertainty on W , produces the uncertainty on $Z_{\max, \odot}$ and hence the $\pm 3\%$ uncertainty on 59%. Our results for eccentricity and Z_{\max} are consistent with those obtained using Hogg et al. (2005) LSR values: $(U, V, W) = (10.1 \pm 0.5, 4.0 \pm 0.8, 6.7 \pm 0.2)$. Using the Hogg et al. LSR values, $92 \pm 1\%$ of A5–K2 stars within 40 pc have higher eccentricities than the Sun and $62 \pm 4\%$ of A5–K2 stars within 40 pc have larger Z_{\max} values.

How does the Sun’s distance from the center of the Milky Way compare to the distances of other stars from the center of the Milky Way? In Fig. 8 we show the distribution of the mean radial distances of stars from the Galactic center, based on the star count model of Bahcall & Soneira (1980). To represent the entire Galactic stellar population we include the disk (thin + thick) and spheroidal (bulge + halo) components. Using the current Solar distance from the center ($R_0 = 7.62 \pm 0.32$ kpc, Eisenhauer et al. 2005) and a disk scale length $h = 3.0 \pm 0.4$ kpc (Gould et al. 1996), we estimate that the Sun lies farther from the Galactic center than $72_{-5}^{+8}\%$ of the stars in the Galaxy. The uncertainty on the result comes from the 68% bounds of the total distribution, which come from the scale length uncertainty (± 0.4 kpc).

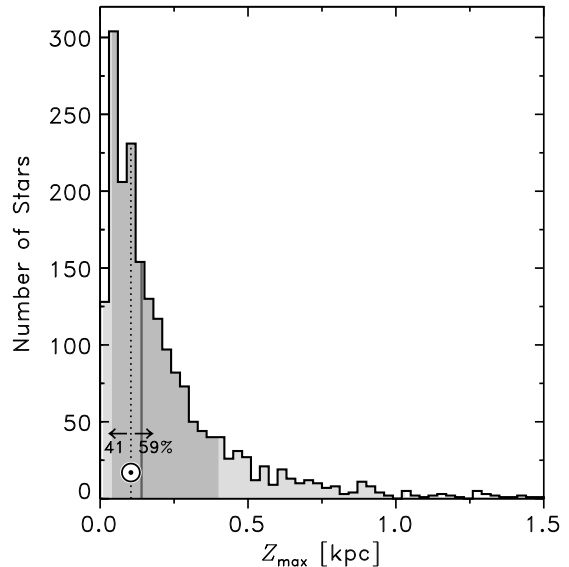


FIG. 7.— The distribution of maximum heights above the Galactic plane for the Nordström et al. (2004) sample. $59 \pm 3\%$ of nearby A5–K2 stars ($d_{\max} = 40$ pc) reach higher above the Galactic plane than the Sun reaches. There are 22 stars evenly distributed over Z_{\max} between 1.5 and 9.6 kpc. Their exclusion from the comparison reduces the 59% result by less than 1%.

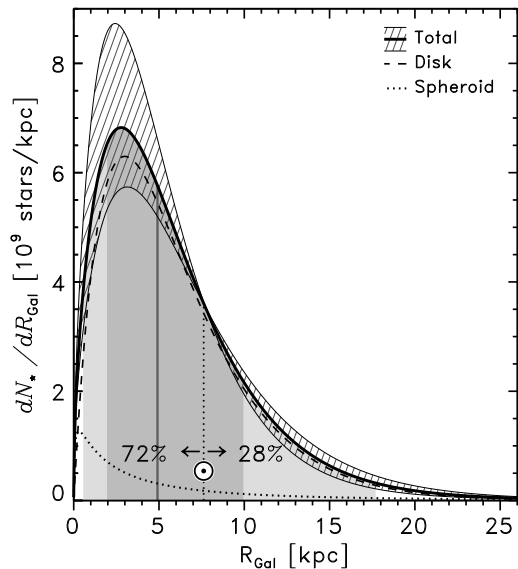


FIG. 8.— Mean stellar galactocentric radius distribution dN_*/dR_{Gal} . The solid curve represents the sum of the disk (dashed line) and spheroidal (dotted line) stellar components. The 68% uncertainty of the total distribution is shown by the cross-hatched area. The Sun is farther from the Galactic center than $72_{-5}^{+8}\%$ of the stars in the Galaxy.

2.7. Host Galaxy Mass

The mass of a star’s host galaxy may be correlated with parameters that have an influence on habitability. For example, galaxy mass affects the overall metallicity distribution that a star would find around itself — an effect that would not show up in Fig. 3, which only shows the local metallicity distribution.

The Milky Way is more massive than $\sim 99\%$ of all galaxies — the precise fraction depends on the lower

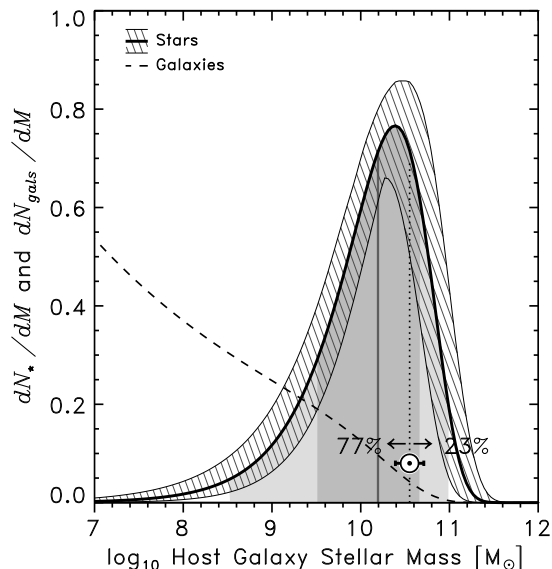


FIG. 9.— Fraction of all stars that live in galaxies of a given mass, dN_*/dM (solid curve). The mass of the Sun’s galaxy is indicated by the “☉”. This distribution represents the amount of stellar mass contributed by galaxies of a given mass. Approximately $77_{-14}^{+11}\%$ of stars live in galaxies less massive than ours. The cross-hatched band shows the 1σ uncertainty associated with the uncertainty in the two Schechter function parameters, α and L^* (Loveday 2000; Schechter 1976). The dashed line shows the unweighted luminosity function (the number of galaxies per luminosity interval dN_{gals}/dM) according to which the Milky Way is more massive than $\sim 99\%$ of galaxies.

galaxy, and the behaviour of the low-mass end of the galaxy mass function (Silk 2007). We are referring here to the stellar mass, not the total baryonic mass or the total mass. Despite the Milky Way’s large mass compared to other galaxies, if most stars in the Universe resided in even more massive galaxies, the Milky Way would be a rather low mass galaxy for a star to belong to. To estimate the fraction of all stars in galaxies of a given mass, we first estimate the distribution of galaxy masses by taking the K -band luminosity function of Loveday (2000) (K -band most closely reflects stellar mass since it is less sensitive than other bands to differences in stellar populations) and weighting it by luminosity. We convert this to stellar mass assuming a constant stellar-mass-to-light ratio of 0.5 (Bell & de Jong 2001). This function, plotted in Fig. 9, shows the amount of stellar mass contributed by galaxies of a given mass — or assuming identical stellar populations — the fraction of stars residing in galaxies of a given stellar mass.

We estimate the K -band luminosity of the Milky Way by converting the published V -band magnitude of Courteau & van den Bergh (1999) to the K -band assuming the mean color of an Sbc spiral galaxy from the 2MASS Large Galaxy Atlas (Jarrett et al. 2003) and applying the color conversion from (Driver et al. 1994). We then convert this to stellar mass using the same stellar-mass-to-light ratio used above, i.e., 0.5. In this way we estimate the stellar-mass content of the Milky Way to be $10^{10.55 \pm 0.16} = 3.6_{-1.1}^{+1.5} \times 10^{10} M_\odot$ (see also Flynn et al. 2006). Comparing this to the stellar masses of other galaxies (Fig. 9) we find that $77_{-14}^{+11}\%$ of stars reside in

2.8. Host Group Mass

The mass of a star’s host galactic group or galactic cluster may be correlated with parameters that have an influence on habitability. For example, group mass is correlated with the density of the galactic environment (number of galaxies per Mpc^3) that could, like galactocentric radius, be associated with the dangers of high stellar densities: “The presence of a giant elliptical at a distance of 50 kpc would have disrupted the Milky Way Galaxy, so that human beings (and hence astronomers) probably would not have come into existence.” (van den Bergh 2000). Our Local Group of galaxies seems rather typical (van den Bergh 2000) but we would like to quantify this. Proceeding similarly to our analysis of galaxy mass in Sect. 2.7, we ask, what fraction of stars live in galactic groups less massive than our Local Group? Figure 10 shows the luminosity-weighted (i.e. stellar mass-weighted) number density of galactic groups. The number distribution and luminosity distribution of galactic groups is taken from the Two-degree Field Galaxy Redshift Survey Percolation-Inferred Galaxy Group (2PIGG) catalogue (Eke et al. 2004). It spans the range from weak groups to rich galaxy clusters.

We estimated the stellar masses of the 2PIGG groups and Local Group galaxies (Courteau & van den Bergh 1999) by converting from the B -band assuming a constant stellar-mass-to-light ratio of 1.5 (Bell & de Jong 2001). This gives an estimated stellar mass of the local group of $10^{10.91 \pm 0.07} = 8.1_{-1.2}^{+1.4} \times 10^{10} M_\odot$. Figure 10 indicates that our Local Group is a typical galactic grouping for a star to be part of. Approximately $58 \pm 5\%$ of stars live in galactic groups more massive than our Local Group. With respect to the mass of its galaxy and the mass of its galactic group, the Sun is a fairly typical star in the Universe.

3. JOINT ANALYSIS OF 11 SOLAR PROPERTIES

3.1. Solar χ^2 -Analysis

We would like to know whether the solar properties, taken as a group, are consistent with noise, i.e., are they consistent with the values of a star selected at random from our stellar distributions. We take a χ^2 approach to answering this question. First we estimate the solar χ_\odot^2 , by adding in quadrature, for all 11 properties, the differences between the solar values and the median stellar values. We find:

$$\chi_\odot^2 = \sum_{i=1}^{N=11} \frac{(x_{\odot,i} - \mu_{1/2,i})^2}{\sigma_{68,i}^2} = 7.88_{-0.30}^{+0.08} \quad (1)$$

where i is the property index, $N = 11$ is the number of properties we are considering, $\mu_{1/2,i}$ is the median of the i^{th} stellar distribution and $\sigma_{68,i}$ is the difference between the median and the upper or lower 68% zone, depending on whether the solar value $x_{\odot,i}$ is above or below the median. The uncertainty on χ_\odot^2 is obtained using the uncertainties of $x_{\odot,i}$.

Equation (1) can be improved on by taking into account *i*) the non-Gaussian shapes of the stellar distributions and *ii*) the larger uncertainties of the medians of smaller samples (our smallest sample is ~ 100 stars).

We employ a bootstrap analysis (Efron 1970) to ran-

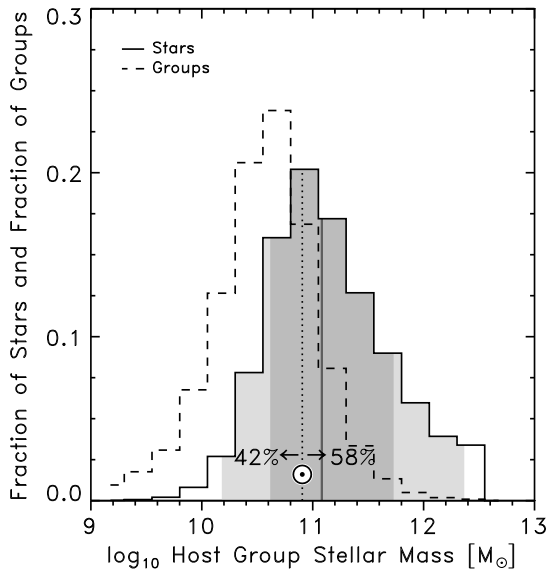


FIG. 10.— The dashed histogram shows the luminosity function of galactic groups (number of groups per interval of B-band luminosity). The solid histogram shows the luminosity-weighted group luminosity function (approximately the fraction of stars which inhabit a group of given stellar mass). The horizontal axis has been converted to stellar mass assuming a constant B-band stellar-mass-to-light ratio of 1.5 (Bell & de Jong 2001). The “ \odot ” shows the estimated mass of the Local Group (Courteau & van den Bergh 1999) and lies just below the median (vertical grey line).

more accurate estimate of χ_{\odot}^2 . Because the bootstrap is a non-parametric method, the distributions need not be Gaussian.

We obtain $\chi_{\odot}^2 = 8.39 \pm 0.96$. Figure 11 shows the resulting solar χ^2 distribution. The median of this distribution is our adopted solar χ^2 value. Dividing our adopted solar χ^2 by the number of degrees of freedom gives our adopted reduced solar χ^2 value:

$$\chi_{\odot}^2/11 = 0.76 \pm 0.09 \quad (2)$$

The standard conversion of this into a probability of finding a lower χ^2 value (assuming normally distributed independent variables) yields:

$$P(< \chi_{\odot}^2 = 8.39 | N = 11) = 0.32 \pm 0.09. \quad (3)$$

3.2. Estimate of $P(< \chi_{\odot}^2)$

To quantify how typical the Sun is with respect to our 11 properties, we compare the solar $\chi_{\odot}^2 (= 8.39)$ to the distribution of χ^2 values obtained from the other stars in the samples.

We perform a Monte Carlo simulation (Metropolis & Ulam 1949) to calculate an estimate of each star’s χ^2 value (χ_{*}^2). The histogram shown in Figure 12 is the resulting Monte Carlo stellar χ^2 distribution. Three standard χ^2 distributions have been over-plotted for comparison ($N = 10, 11, 12$). The probability of finding a star with χ^2 lower than or equal to solar is:

$$P_{\text{MC}}(\leq \chi_{\odot}^2 = 8.39 | N = 11) = 0.29 \pm 0.11 \quad (4)$$

The Monte Carlo χ^2 distribution has a similar shape to the standard χ^2 distribution function for $N = 11$.

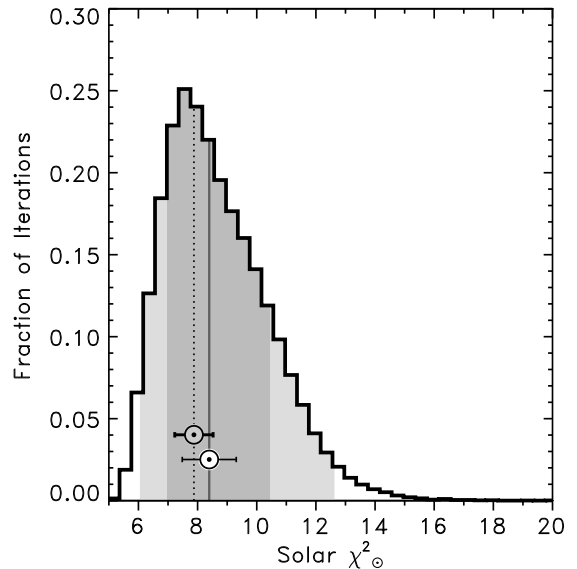


FIG. 11.— Bootstrapped solar χ^2 distribution. The median of the distribution (white “ \odot ”) is $\chi_{\odot}^2 = 8.39 \pm 0.96$. This should be compared to the solar χ_{\odot}^2 value from Eq. 1: $7.88_{-0.30}^{+0.08}$ which is over-plotted (grey “ \odot ” on dotted line).

$0.29 \sim P(\leq \chi^2) = 0.32$ (Eqs. 3 and 4). The more appropriate Monte Carlo distribution has a longer tail, produced by the longer super-Gaussian tails of the stellar distributions.

Table 2 summarizes our analysis for the solar χ_{\odot}^2 values and the probabilities $P(< \chi_{\odot}^2)$. Our simple $\chi_{\odot}^2 = 7.88$ estimate increased to 8.39 and the uncertainty increased by a factor of ~ 3 after non-Gaussian and sample size effects were included as additional sources of uncertainty. Our improved analysis yields $P_{\text{MC}}(\leq \chi_{\odot}^2)$, with a longer tail and brings the probability down from 0.32 ± 0.09 to 0.29 ± 0.11 . If this value were close to 1, almost all other stars would have lower χ^2 values and we would have good reason to suspect that the Sun is not a typical star. However, this preliminary low value of 0.29 indicates that if a star is chosen at random, the probability that it will be more typical (\sim have a lower χ^2 value) than the Sun (with respect to the 11 properties analysed here), is only $29 \pm 11\%$. The details of our improved estimates of χ_{\odot}^2 and $P(< \chi_{\odot}^2)$ can be found in the Appendix 6.

4. RESULTS

Figure 13 shows four different representations of our results. Figure 13A compares the solar values to each stellar distribution’s median and 68% and 95% zones. The Sun lies beyond the 68% zone for three properties: mass (95%), eccentricity (93%) and rotational velocity (88%). No solar property lies beyond the 95% zone. The histogram in Figure 13B is the distribution of solar values in units of standard deviations:

$$z_i = \frac{x_{\odot,i} - \mu_{1/2,i}}{\sigma_{68,i}} \quad (5)$$

For each stellar property i , the Sun has a larger value than $n_i\%$ of the stars. If the Sun were a randomly selected star, we would expect the percentages $n_i\%$ to be scattered roughly evenly between 0% and 100%.

TABLE 2
SUMMARY OF χ^2 AND $P(< \chi^2_{\odot})$ RESULTS.

Analysis	χ^2_{\odot}	$\chi^2_{\odot}/11$	$P(< \chi^2_{\odot} N = 11)$	$P_{\text{MC}}(< \chi^2_{\odot} N = 11)$
simple	$7.88^{+0.08}_{-0.30}$ (Eq. 1)	$0.72^{+0.01}_{-0.03}$	$0.28^{+0.01}_{-0.03}$ (Eq. 7)	—
improved	8.39 ± 0.96	0.76 ± 0.09 (Eq. 2)	0.32 ± 0.09 (Eq. 3)	0.29 ± 0.11 (Eq. 4)

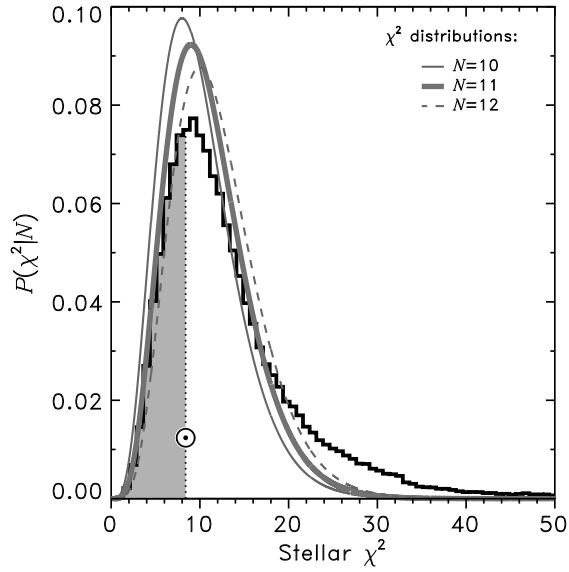


FIG. 12.— Stellar χ^2 distribution from our Monte Carlo simulation. $P_{\text{MC}}(< \chi_{\odot}^2 = 8.39) = 0.29 \pm 0.11$ (represented by the grey shade) is calculated integrating from $\chi^2 = 0$ to $\chi^2 = \chi_{\odot}^2$. For comparison, three χ^2 distribution-curves are over-plotted with 10, 11, and 12 degrees of freedom. The standard probability from the $N = 11$ curve yields: $P(< \chi_{\odot}^2 = 8.39|N = 11) = 0.32 \pm 0.09$.

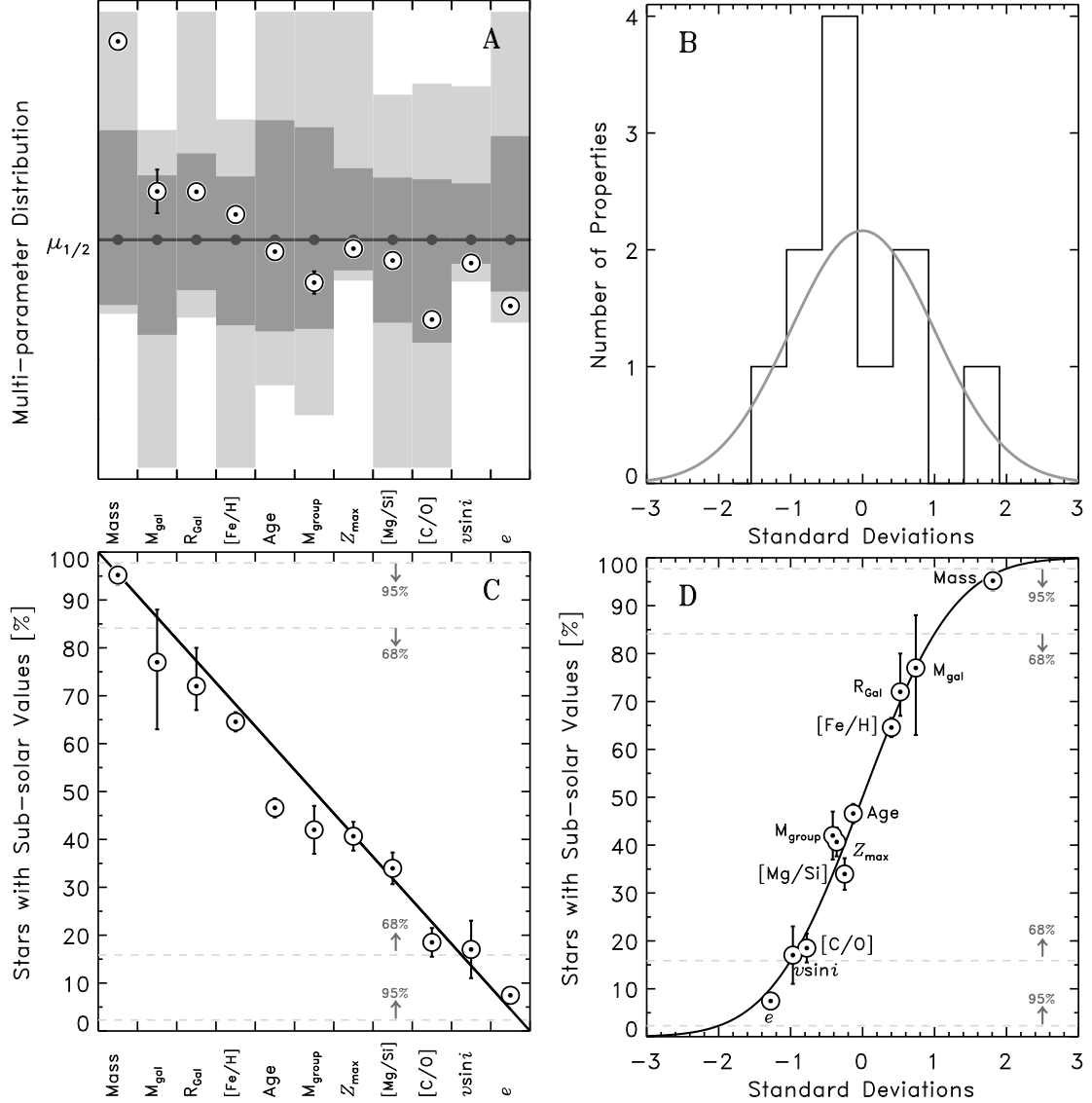


FIG. 13.— Various representations of our main results. **A:** Solar values of 11 properties compared to the distribution for each property. Each distribution’s median value is indicated by a small filled circle. The dark and light grey shades represent the 68% and 95% zones respectively. **B:** Histogram of the number of properties as a function of the number of standard deviations the solar value is from the median of that property. The grey curve is a Gaussian probability distribution normalised to 11 parameters. **C:** Percentage n_i of stars with sub-solar values as a function of property. The average signal expected from a random star is shown by the solid line (see Sec. 4). **D:** Percentage n_i of stars with sub-solar values as a function of the number of standard deviations the solar value is from the median of that property. The solid curve is a cumulative Gaussian distribution — if every sample were a Gaussian distribution, every solar dot would sit exactly on the line. Just as in (C), the dashed lines encompass the 68% and 95% zones. Similar to the results from Figure 12, these four panels indicate that the Sun is a typical star.

When the $n_i\%$ values are lined up in decreasing order (Fig. 13C), we expect them to be near the line given by:

$$n_{i,\text{expected}}\% = \left[1 - \frac{(i-1/2)}{N} \right] \times 100\% \quad (6)$$

and plotted in Figure 13C. Any anomalies would show up as points ‘ \odot ’ significantly distant from the line.

Figure 13D compares the percentages $n_i\%$ of stars having sub-solar values (shown in Figure 13C) with the solar values expressed in units of standard deviations from each distribution’s median (shown in Fig. 13B). If the stellar distributions were perfect Gaussians, the translation from z_i to n_i would be given by the cumulative Gaussian distribution (Fig. 13D, *solid curve*). That the points lie along this line demonstrates that the approximation of our distributions as Gaussians is reasonable.

Table 3 lists percentages $n_i\%$ of stars for each property (as shown in Fig. 13). In the lower half of the table we list properties not included in this analysis because of correlations with properties that are included.

Individual stellar uncertainties make the observed characteristic widths (σ_{68} , Table 1) larger than the widths of the intrinsic distributions. This broadening effect makes the Sun appear more typical than it really is when σ_{68} and the individual stellar uncertainties (σ_*) are of similar size and the individual stellar uncertainties are much larger than the solar uncertainty (σ_\odot). We estimate that our results are not significantly affected by this broadening effect.

Our resulting probability of finding a star with a χ^2 lower or equal to the solar value of $29 \pm 11\%$ (Eq. 4), is consistent with the probability we would obtain if stellar multiplicity were included in our study. Using the volume limited sample used for stellar mass in Section 2.1 (125 A1–M7 stars within 7.1 pc) the probability that a randomly selected star will be single is $52.8 \pm 4.5\%$, which means that \sim half of stars are single while the other half have one or more companions. Including this in our bootstrap analysis and Monte Carlo simulations (see Appendix 6) marginally increases the probability in Eq. 4 to $33 \pm 11\%$. If the multiplicity data for 246 G dwarfs from Duquennoy & Mayor (1991) is used instead — the probability that a randomly selected G dwarf will be single is $37.8 \pm 2.9\%$ — then the probability in Eq. 4 would increase to $34 \pm 11\%$. The inclusion of stellar multiplicity marginally increases our reported probability.

In Figures 6 and 7 of Radick et al. (1998), the Sun’s short-term variability as a function of average chromospheric activity, appears $\sim 1\sigma$ low, compared to a distribution of 35 F3–K7 Sun-like stars (Lockwood et al. 1997). Lockwood et al. (2007) suggest that the Sun’s small total irradiance variation compared to stars with similar mean chromospheric activity, may be due to their limited sample and the lack of solar observations out of the Sun’s equatorial plane. We do not include short or long term variability (chromospheric or photometric) in Table 3 because of the small size of the Lockwood et al. (2007) sample. We also do not include the chromospheric index R'_{HK} (see Table 3, bottom panel) as one of our 11 properties because of its correlation with the chromospheric ages of our sample.

5. DISCUSSION AND INTERPRETATION

The probability $P_{\text{MC}}(\leq \chi^2_\odot) = 0.29 \pm 0.11$ classifies the Sun as a typical star. How robust is this result? The probability of finding a star with a χ^2 lower than or equal to χ^2_\odot , depends on the properties selected for the analysis (see problem *iii* of Section I). For example, if we had chosen to consider only mass and eccentricity data, this analysis would yield $P_{\text{MC}}(\chi^2 \leq \chi^2_\odot) = 0.94 \pm 0.4$, i.e., the Sun would appear mildly ($\sim 2\sigma$) anomalous. If on the other hand, we had chosen to remove mass and eccentricity from the analysis, we would obtain $P_{\text{MC}}(\chi^2 \leq \chi^2_\odot) = 0.07 \pm 0.04$, which is anomalously low. The most common cause of such a result is the over-estimation of error bars. The next most common cause is the preselection of properties known to have $n_i\% \sim 50\%$.

Gustafsson (1998) discussed the atypically large solar mass, and proposed an anthropic explanation — the Sun’s high mass is probably related to our own existence. He suggested that the solar mass could hardly have been greater than $\sim 1.3 M_\odot$ since the main sequence lifetime of a $1.3 M_\odot$ star is ~ 5 billion years (Clayton 1983). He also discussed how the dependence of the width of the circumstellar habitable zone on the host star’s mass probably favours host stars within the mass range $0.8\text{--}1.3 M_\odot$.

Our property selection criteria is to have the largest number of maximally independent properties that have a plausible correlation with habitability and, ones for which a representative stellar sample could be assembled. Our joint analysis does not weight any parameter more heavily than any other. If the only properties associated with habitability are mass and eccentricity then we have diluted a $\sim 2\sigma$ signal that would be consistent with Gustafsson’s proposed anthropic explanation.

Our analysis points in another direction. If mass and eccentricity were the only properties associated with habitability, then the solar values for the remaining nine properties would be consistent with noise. However, a joint analysis of just the remaining nine properties produces a $\chi^2_{\odot,9} = 3.6 \pm 0.4$ and the anomalously low probability: $P(\leq \chi^2_{\odot,9}) = 0.07 \pm 0.04$, which suggests that the nine properties are unlikely to be the properties of a star selected at random with respect to these properties.

The χ^2 fit of the 11 points in Panel C of Fig. 13 to the diagonal line yields a fit that is substantially better than the fit of the remaining nine properties to Eq. 7 with $N = 9$. In other words, the joint analysis suggests that although mass and eccentricity are the most anomalous solar properties, it is unlikely that they are associated with habitability, because without them, it is unlikely that the remaining solar properties are just noise. Thus, the Sun, despite its mildly ($\sim 2\sigma$) anomalous mass and eccentricity, can be considered a typical, randomly selected star.

There may be stellar properties crucial for life that were not tested here. If we have left out the most important properties, with respect to which the Sun is atypical, then our Sun-is-typical conclusion will not be valid. If we have sampled all properties associated with habitability, our Sun-is-typical result suggests that there are no special requirements on a star for it to be able to host a planet with life.

TABLE 3
SUMMARY OF HOW THE SUN COMPARES TO OTHER STARS (SEE FIG. 13)

Parameter	Figure	$n_i\%$	Level of Anomaly
Mass	1	$95 \pm 2\%$	of nearby stars are less massive than the Sun.
Age	2	$53 \pm 2\%$	of stars in the thin disk of the Galaxy are older than the Sun.
[Fe/H]	3	$65 \pm 2\%$	of nearby stars are more iron-poor than the Sun.
[C/O]	4A	$81 \pm 3\%$	of nearby stars have a higher C/O ratio than the Sun.
[Mg/Si]	4B	$66 \pm 3\%$	of nearby stars have a higher Mg/Si ratio than the Sun.
$v \sin i$	5	$83 \pm 7\%$	of nearby Sun-like-mass stars rotate faster than the Sun.
e	6	$93 \pm 1\%$	of nearby stars have larger galactic orbital eccentricities than the Sun.
Z_{\max}	7	$59 \pm 3\%$	of nearby stars reach farther from the Galactic plane than the Sun.
R_{Gal}	8	$72^{+8}_{-5}\%$	of stars in the Galaxy are closer to the galactic center than the Sun.
M_{gal}	9	$77^{+11}_{-14}\%$	of stars in the Universe are in galaxies less massive than the Milky Way.
M_{group}	10	$58 \pm 5\%$	of stars in the Universe are in groups more massive than the local group.
Properties Not Included in the Analysis Because They Are Correlated with the Selected 11 Parameters			
Mass: IMF _{Stellar}	1	$94 \pm 2\%$	of nearby stars are less massive than the Sun.
Age: SFR _{Cosmic}	2	$86 \pm 5\%$	of stars in the Universe are older than the Sun.
Age ^a	—	$55 \pm 2\%$	of nearby Sun-like-mass stars are older than the Sun.
[Fe/H] ^b	—	$56 \pm 5\%$	of nearby stars are more iron-poor than the Sun.
$v \sin i$ ^c	—	$92 \pm 5\%$	of nearby Sun-like-mass stars rotate faster than the Sun.
$\log R'_{\text{HK}}$ ^d	—	$51 \pm 2\%$	of nearby FGKM stars are more chromospherically active.
[O/Fe]	—	$75 \pm 3\%$	of nearby stars have a lower O/Fe ratio than the Sun.
R_{\min}	—	$91 \pm 1\%$	of nearby stars get closer to the Galactic center.
v_{LSR}	—	$93 \pm 1\%$	of nearby stars have smaller velocity with respect to the LSR.
$ U $	—	$75 \pm 1\%$	of nearby stars have larger absolute radial velocity.
$ V $	—	$82 \pm 1\%$	of nearby stars have larger absolute tangential velocity.
$ W $	—	$58 \pm 1\%$	of nearby stars have larger absolute vertical velocity.

^a 1126 stars (A5–K2) from Nordström et al. (2004).

^b 91 stars (GK) from Favata et al. (1997).

^c 590 stars (F8–K2) from Nordström et al. (2004).

^d 866 stars (FGKM) from Wright et al. (2004).

6. CONCLUSIONS

We have compared the Sun to representative stellar samples for 11 properties. Our main results are as follows:

- Stellar mass and Galactic orbital eccentricity are the most anomalous properties. The Sun is more massive than $95 \pm 2\%$ of nearby stars and has a Galactic orbital eccentricity lower than $93 \pm 1\%$ FGK stars within 40 pc.
- Our joint bootstrap analysis yields a solar $\chi^2 \chi_{\odot}^2 = 8.39 \pm 0.96$ and a solar reduced $\chi^2 \chi_{\odot}^2/11 = 0.76 \pm 0.09$. The probability of finding a star with a χ^2 lower than or equal to solar $P_{\text{MC}}(\leq \chi_{\odot}^2 = 8.39 \pm 0.96) = 0.29 \pm 0.11$.

To our knowledge, this is the most comprehensive and quantitative comparison of the Sun with other stars. We find that taking all 11 properties together, the Sun is a typical star. This finding is largely in agreement with Gustafsson (1998), however our results undermine the proposition that an anthropic explanation is needed for the comparatively large mass of the Sun.

Further work could encompass the inclusion of other properties potentially associated with habitability. Another improvement would come when larger stellar samples become available for which all properties could be derived, instead of using different samples for different properties as was done here. In addition, research in the molecular evolution that led to the origin of life may, in the future, be able to provide more clues as to which

on Earth, orbiting the Sun.

Acknowledgments: We would like to thank Charles Jenkins for clarifying discussions of statistics, particularly on how to include stellar multiplicity, and Martin Asplund and Jorge Meléndez for discussions of elemental abundances. JAR acknowledges an RSAA PhD research scholarship. MP acknowledges the financial support of the Australian Research Council. EG acknowledges the financial support of the Finnish Cultural Foundation.

APPENDIX A

PROPERTY CORRELATIONS

The χ^2 formalism and the use of the χ^2 -distribution to obtain $P(< \chi_{\odot}^2|N)$, — improved using Monte-Carlo simulations in Section 3.2 to obtain $P_{\text{MC}}(\leq \chi_{\odot}^2)$ — assumes that each parameter is independent of the others. In selecting our 11 properties we have selected properties which are maximally independent based on plotting property 1 vs property 2 for the same stars. We show seven such plots in this Appendix.

If there are correlations between the analysed properties, then the number of degrees of freedom N could drop from 11 to ~ 10.5 (see Fig. 12). Some properties have been excluded from the analysis due to a correlation with another property in the analysis.

A1. ELEMENTAL RATIOS

In Figure 14 we show the distribution for carbon to oxygen ratio [C/O] versus the magnesium to silicon ratio

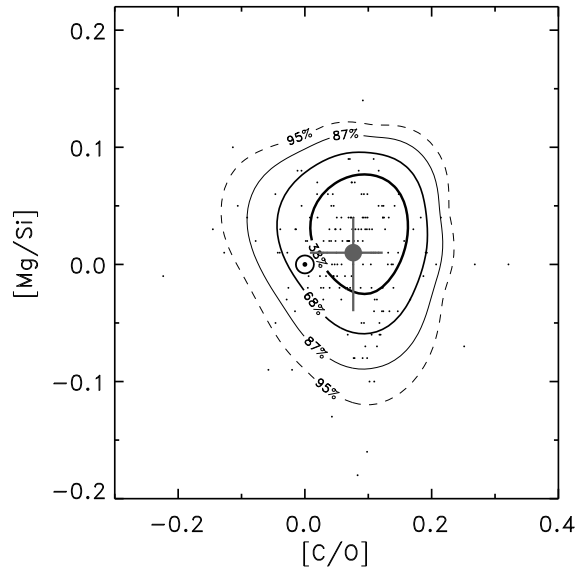


FIG. 14.— Carbon to oxygen ratio [C/O] versus magnesium to silicon ratio [Mg/Si] of 176 FG stars with abundances for these elements (Reddy et al. 2003). In Figs. 4C and 4D we showed that the [C/O] and [Mg/Si] distributions are largely independent of [Fe/H]. Here we show that these distributions are also largely independent of each other. Note that in this comparison we only use the data from Reddy et al. (2003), since it is the largest available sample with C, O, Mg and Si abundances.

A2. MASS, AGE, AND ROTATIONAL VELOCITY

In Figure 15 we show four correlation plots for mass, chromospheric age, rotational velocity and $v \sin i$. We use the stars common to both Wright et al. (2004) and Valenti & Fischer (2005) for which these observables are available.

A3. GALACTIC ORBITAL PARAMETERS

The Galactic orbital eccentricity (e) and the magnitude of the galactic orbital velocities with respect to the local standard of rest (v_{LSR}) are strongly correlated (see Fig. 6 in Sec. 2.6). We selected e instead of v_{LSR} because of its near independence of the maximum height above the galactic plane (Z_{max}); see Figure 16.

APPENDIX B

IMPROVED ESTIMATES OF χ_{\odot}^2 AND $P(< \chi_{\odot}^2)$

In Section 3.2, with 11 degrees of freedom, the reduced χ^2 from Equation 4 is $\chi_{\odot}^2 / 11 = 0.72_{-0.03}^{+0.01}$. Since $\chi_{\odot}^2 / 11 < 1$, the Sun’s properties are consistent with the Sun being a randomly selected star.

To improve on this preliminary analysis (but with a similar conclusion), as mentioned in Section 3.2, we employ a bootstrap analysis (Efron 1979) to randomly resample data (with replacement) and derive a more accurate estimate of χ_{\odot}^2 . Because the bootstrap is a non-parametric method, the distributions need not be Gaussian.

For every iteration, each parameter’s stellar distribution is randomly resampled and a χ_{\odot}^2 value is calculated using Eq. (1). The uncertainties $\sigma_{\odot,i}$ of the solar values $x_{\odot,i}$ are also included in the bootstrap method: for every iteration, the Solar value for each parameter is replaced in Eq. (1) by a randomly selected value from a normal distribution with median $\mu_{\odot,i} = x_{\odot,i}$ and standard de-

although the resulting distribution varies very little once the number of iterations reaches $\sim 10,000$.

The median of this distribution and the error on the median yields our improved value for the reduced χ_{\odot}^2 (Fig. 11). The uncertainty of the median of each resampled distribution varies inversely proportionally to the square root of the number of stars in the distribution, $\Delta\mu_{1/2,i} \propto 1/\sqrt{N_{*,i}}$. In other words, median values are less certain for smaller samples and this uncertainty is included in our improved estimate of χ_{\odot}^2 , and its uncertainty.

We find the probability of finding a star with a χ_{\star}^2 value lower than the solar χ_{\odot}^2 , for $N = 11$ degrees of freedom in the standard way (Press et al. 1992) and obtain:

$$P(< \chi_{\odot}^2 = 7.88_{-0.30}^{+0.08} | 11) = 0.28_{-0.03}^{+0.01} \quad (7)$$

To improve our estimate of the probability of finding a star with lower χ^2 value than the Sun, we perform a Monte Carlo simulation (Metropolis & Ulam 1949) to calculate an estimate of each star’s χ^2 value (χ_{\star}^2). For every iteration, we randomly select a star from each stellar distribution. We then calculate its χ_{\star}^2 value by replacing the solar value $x_{\odot,i}$ with that star’s value $x_{*,i}$ in Eq. (1). This process was repeated 100,000 times to create our Monte Carlo stellar χ^2 distribution. Stars were randomly selected with replacement, thus the simulated χ^2 distribution accounts for small number statistics and non-Gaussian distributions. The probability of finding a star with χ^2 lower than or equal to solar is $P_{\text{MC}} = 0.29 \pm 0.11$.

The results of our analysis for the Solar χ_{\odot}^2 values and the probabilities $P(< \chi_{\odot}^2)$ are summarized in Table 2

B1. ADDITION OF A DISCRETE PARAMETER

In Section 4 we discuss the addition of stellar multiplicity to our analysis. Since stellar multiplicity cannot easily be approximated by a one-sided Gaussian (particularly because the Sun is on the edge of the distribution, i.e., it is of multiplicity one), we modified our Monte Carlo procedure to include this discrete parameter. The likelihood of observing a particular χ^2 for the 11 parameters is

$$\exp\left(-\frac{1}{2} \sum_{i=1}^{11} \chi_i^2\right). \quad (8)$$

We take the probability $p(1)$ of a star being a single star, to be $53.8 \pm 4.5\%$, obtained from our sample of nearby stars (Sec. 2.1). The likelihood L of observing a particular χ^2 and $p(1)$ is the product

$$L = p(1) \exp\left(-\frac{1}{2} \sum_{i=1}^{11} \chi_i^2\right). \quad (9)$$

Taking logarithms we can then compute the distribution of the statistic S , where

$$S = \ln p(1) - \frac{1}{2} \sum_{i=1}^{11} \chi_i^2. \quad (10)$$

The distribution of S allows us to obtain the results for

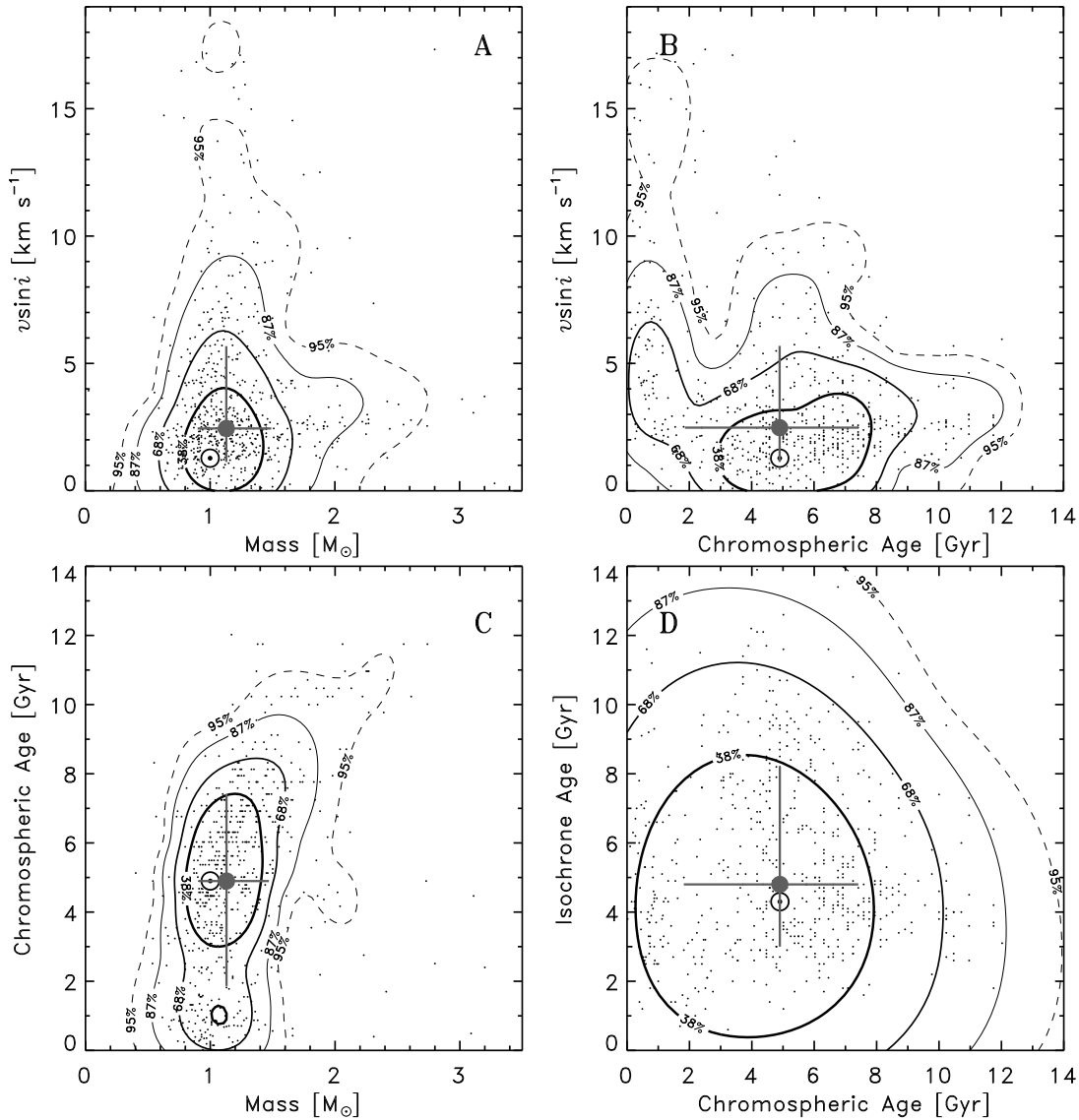


FIG. 15.— Correlation plots between various properties. For all four panels we use the stars common to both Wright et al. (2004) and Valenti & Fischer (2005). Panel (A): mass vs rotational velocity $v \sin i$ for 713 FGK stars. This panel shows the degree of correlation between mass and $v \sin i$. See Gray (2005) for a stronger correlation between these two variables when a larger mass range and more active stars are kept in the sample. To minimize the effect of this correlation on our analysis, we restrict the range of mass in Fig. 5 to 0.9 to $1.1M_{\odot}$. Panel (B): chromospheric age versus $v \sin i$ for 641 FGK stars. The lack of correlation between chromospheric determined ages and rotational velocities is shown. Panel (C): no strong correlation between mass and chromospheric age for 639 FGK stars. Panel (D): the ages of 637 stars determined by the chromospheric method versus their ages from the isochrone method.

REFERENCES

- Allègre, C. J., Manhès, G., & Göpel, C. 1995, *Geochim. Cosmochim. Acta*, 59, 1445
- Allende Prieto, C. 2006, *ArXiv Astrophysics e-prints*
- Allende Prieto, C., Lambert, D. L., & Asplund, M. 2001, *ApJ*, 556, L63
- Asplund, M., Grevesse, N., & Sauval, A. J. 2005, in *ASP Conf. Ser. 336: Cosmic Abundances as Records of Stellar Evolution and Nucleosynthesis*, 25
- Bahcall, J. N., & Soneira, R. M. 1980, *ApJS*, 44, 73
- Bell, E. F., & de Jong, R. S. 2001, *ApJ*, 550, 212
- Bensby, T., & Feltzing, S. 2006, *MNRAS*, 367, 1181
- Bensby, T., Feltzing, S., Lundström, I., & Ilyin, I. 2005, *A&A*, 433, 185
- Bertelli, G., & Nasi, E. 2001, *AJ*, 121, 1013
- Carter, B. 1983, *Philos. Trans. R. Soc. London*, A, 310
- Clayton, D. D. 1983, *Principles of stellar evolution and nucleosynthesis* (Chicago: University of Chicago Press, 1983)
- Driver, S. P., Philipps, S., Davies, J. I., Morgan, I., & Disney, M. J. 1994, *MNRAS*, 268, 393
- Duquennoy, A., & Mayor, M. 1991, *A&A*, 248, 485
- Edvardsson, B., Andersen, J., Gustafsson, B., Lambert, D. L., Nissen, P. E., & Tomkin, J. 1993a, *A&A*, 275, 101
- . 1993b, *A&AS*, 102, 603
- Efron, B. 1979, *The Annals of Statistics*, 7, 1
- Eisenhauer, F. et al. 2005, *ApJ*, 628, 246
- Eke, V. R. et al. 2004, *MNRAS*, 355, 769
- Favata, F., Micela, G., & Sciortino, S. 1996, *A&A*, 311, 951
- . 1997, *A&A*, 323, 809
- Feltzing, S., Holmberg, J., & Hurley, J. R. 2001, *A&A*, 377, 911
- Flynn, C., Holmberg, J., Portinari, L., Fuchs, B., & Jahreiß, H. 2006, *MNRAS*, 372, 1149
- Flynn, C., Sommer-Larsen, J., & Christensen, P. R. 1996, *MNRAS*, 281, 1027
- Fuhrmann, K. 2008, *MNRAS*, 384, 173
- Gray, R. O. 2005, *MNRAS*, 362, 17

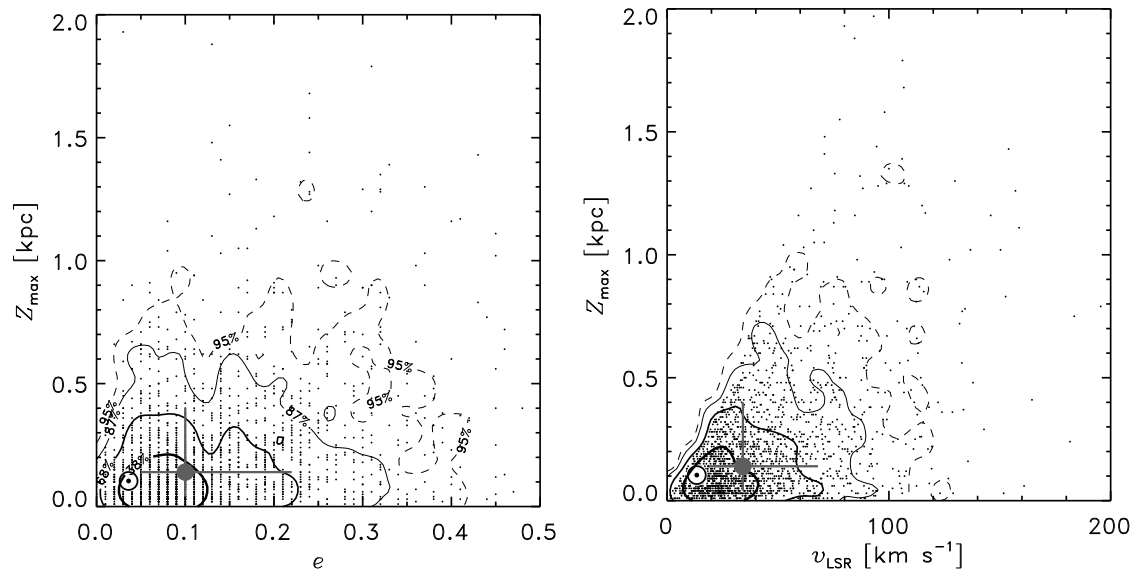


FIG. 16.— Left panel: Galactic orbital eccentricity e versus Z_{\max} for 1987 FGK stars within 40 pc (Nordström et al. 2004). The orbital eccentricity is not correlated with Z_{\max} . Right panel: v_{LSR} versus Z_{\max} for the same stars. Because v_{LSR} is more strongly correlated with Z_{\max} than eccentricity, eccentricity has been selected for the joint analysis instead of v_{LSR} . As in Fig. 4, the contours correspond to 38%, 68%, 82% and 95%.

- Gonzalez, G., Brownlee, D., & Ward, P. 2001, *Icarus*, 152, 185
- Gould, A., Bahcall, J. N., & Flynn, C. 1996, *ApJ*, 465, 759
- Gray, D. F. 2005, *The Observation and Analysis of Stellar Photospheres (The Observation and Analysis of Stellar Photospheres, 3rd Edition, by D.F. Gray. ISBN 0521851866. http://www.cambridge.org/us/catalogue/catalogue.asp?isbn=0521851866. Cambridge, UK: Cambridge University Press, 2005.)*
- Grether, D., & Lineweaver, C. H. 2006, *ApJ*, 640, 1051
- 2007, *ApJ*, 669, 1220
- Gustafsson, B. 1998, *Space Science Reviews*, 85, 419
- Gustafsson, B., Karlsson, T., Olsson, E., Edvardsson, B., & Ryde, N. 1999, *A&A*, 342, 426
- Henry, T. J. 2006, RECONS database
- Hernandez, X., Valls-Gabaud, D., & Gilmore, G. 2000, *MNRAS*, 316, 605
- Hogg, D. W., Blanton, M. R., Roweis, S. T., & Johnston, K. V. 2005, *ApJ*, 629, 268
- Hopkins, A. M., & Beacom, J. F. 2006, *ApJ*, 651, 142
- Jarrett, T. H., Chester, T., Cutri, R., Schneider, S. E., & Huchra, J. P. 2003, *AJ*, 125, 525
- Kasting, J. F., Whitmire, D. P., & Reynolds, R. T. 1993, *Icarus*, 101, 108
- Kroupa, P. 2002, *Science*, 295, 82
- Kroupa, P., & Weidner, C. 2005, in *ASSL Vol. 327: The Initial Mass Function 50 Years Later*, ed. E. Corbelli, F. Palla, & H. Zinnecker, 175
- Kuchner, M. J., & Seager, S. 2005, *ArXiv Astrophysics e-prints*
- Lineweaver, C. H., Fenner, Y., & Gibson, B. K. 2004, *Science*, 303, 59
- Lockwood, G. W., Skiff, B. A., Henry, G. W., Henry, S., Radick, R. R., Baliunas, S. L., Donahue, R. A., & Soon, W. 2007, *ApJS*, 171, 260
- Lockwood, G. W., Skiff, B. A., & Radick, R. R. 1997, *ApJ*, 485, 789
- Loveday, J. 2000, *MNRAS*, 312, 557
- Metropolis, N., & Ulam, S. 1949, *Journal of the American Statistical Association*, 44, 335
- Metzger, M. R., Caldwell, J. A. R., & Schechter, P. L. 1998, *AJ*, 115, 635
- Meyer, S. L. 1975, *Data Analysis for Scientists and Engineers (Data Analysis for Scientists and Engineers, by Stuart L. Meyer p. 186. ISBN 0471599956. NY, USA: John Wiley & Sons, 1975.)*
- Nordström, B. et al. 2004, *A&A*, 418, 989
- Press, W. H., Teukolsky, S. A., Vetterling, W. T., & Flannery, B. P. 1992, *Numerical recipes in FORTRAN. The art of scientific computing (Cambridge: University Press, —c1992, 2nd ed.)*
- Radick, R. R., Lockwood, G. W., Skiff, B. A., & Baliunas, S. L. 1998, *ApJS*, 118, 239
- Ramírez, I., Allende Prieto, C., & Lambert, D. L. 2007, *A&A*, 465, 271
- Reddy, B. E., Tomkin, J., Lambert, D. L., & Allende Prieto, C. 2003, *MNRAS*, 340, 304
- Reid, I. N. 2002, *PASP*, 114, 306
- Reid, I. N., Turner, E. L., Turnbull, M. C., Mountain, M., & Valenti, J. A. 2007, *ApJ*, 665, 767
- Rocha-Pinto, H. J., Maciel, W. J., Scalo, J., & Flynn, C. 2000a, *A&A*, 358, 850
- Rocha-Pinto, H. J., Scalo, J., Maciel, W. J., & Flynn, C. 2000b, *ApJ*, 531, L115
- Schechter, P. 1976, *ApJ*, 203, 297
- Silk, J. 2007, *Astronomy and Geophysics*, 48, 30
- Soderblom, D. R. 1983, *ApJS*, 53, 1
- 1985, *AJ*, 90, 2103
- Truran, Jr., J. W., & Heger, A. 2005, *Origin of the Elements (Meteorites, Comets and Planets: Treatise on Geochemistry, Volume 1)*
- Valenti, J. A., & Fischer, D. A. 2005, *ApJS*, 159, 141
- van den Bergh, S. 2000, *The Galaxies of the Local Group (The galaxies of the Local Group, by Sidney Van den Bergh. Published by Cambridge, UK: Cambridge University Press, 2000 Cambridge Astrophysics Series Series, vol no: 35, ISBN: 0521651816.)*
- Wright, J. T., Marcy, G. W., Butler, R. P., & Vogt, S. S. 2004, *ApJS*, 152, 261